2007

Magnetic anisotropy of deposited transition metal clusters

S. Bornemann
Ludwig-Maximilians-Universitat Munchen, 81377 Munchen, Germany

J. Minar
Ludwig-Maximilians-Universitat Munchen, 81377 Munchen, Germany

J.B. Staunton
Max Planck Institut for Solid State Research, 70569 Stuttgart, Germany

Jan Honolka
Max-Planck-Institut für Festkörperforschung, honolka@fzu.cz

Axel Enders
University of Nebraska at Lincoln, a.enders@me.com

See next page for additional authors

Eur. Phys. J. D **45**, 529–534 (2007)
DOI: 10.1140/epjd/e2007-00190-9

THE EUROPEAN PHYSICAL JOURNAL D

Magnetic anisotropy of deposited transition metal clusters

S. Bornemann[1], J. Minár[1], J.B. Staunton[2], J. Honolka[3], A. Enders[3], K. Kern[3], and H. Ebert[1,a]

[1] Department Chemie und Biochemie, Ludwig-Maximilians-Universität München, 81377 München, Germany
[2] Department of Physics, University of Warwick, Coventry CV4 7AL, UK
[3] Max Planck Institut for Solid State Research, 70569 Stuttgart, Germany

Received 19 April 2007 / Received in final form 5 May 2007
Published online 13 june 2007 –

Abstract. We present results of magnetic torque calculations using the fully relativistic spin-polarized Korringa-Kohn-Rostoker approach applied to small Co and Fe clusters deposited on the Pt(111) surface. From the magnetic torque one can derive amongst others the magnetic anisotropy energy (MAE). It was found that this approach is numerically much more stable and also computationally less demanding than using the magnetic force theorem that allows to calculate the MAE directly. Although structural relaxation effects were not included our results correspond reasonably well to recent experimental data.

PACS. 73.22.-f Electronic structure of nanoscale materials: clusters, nanoparticles, nanotubes, and nanocrystals – 75.30.Et Exchange and superexchange interactions – 75.75.+a Magnetic properties of nanostructures

1 Introduction

In recent years, low-dimensional magnetic nanostructures on surfaces have been the subject of intense experimental and theoretical research activities which are driven by fundamental as well as practical interests. One of the central questions for potential future applications is how the spin-orbit coupling (SOC) induces specific magnetic properties such as orbital magnetic moments and magnetic anisotropy. Another interesting issue is its influence on the exchange coupling. Hereby, it is especially important to understand how these properties evolve from single magnetic adatoms to submonolayer magnetic particles. This very prominent role of SOC for such systems is also reflected in recent reviews [1] as well as theoretical work [2].

A system which has been intensively investigated experimentally [3–10] as well as theoretically [11–15] in recent years is Co/Pt(111) (used here as a short notation for Co clusters or nanostructures, respectively, deposited on a Pt(111) substrate) as this is a prototype to study the requirements on new high-density magnetic storage materials. Earlier theoretical works studied only rather small Co clusters or Co chains on Pt(111) [11–14], whereas only recently first qualitative results and trends based on a parameterised tight-binding approach were published for deposited structures of up to 37 Co atoms [15]. In our earlier works [11–13] on the Co/Pt(111) system we already described the evolution of the spin and orbital moments as well as the exchange coupling for small clusters. What has been missing so far, for a complete picture of the magnetic behaviour is the magnetic anisotropy energy (MAE) for such systems. In principle, calculations of the MAE are possible by applying the magnetic force theorem or by determining the total energies as a function of the magnetisation direction. However, it turned out that these procedures are rather delicate when dealing with deposited clusters and one needs to take great care when taking band or total energy differences. Therefore, we implemented a method to calculate the magnetic torque directly from the electronic structure. Calculating the magnetic torque for a sequence of directions of the magnetisation then gives access to the MAE.

In this present work we show first results for magnetic torque calculations of the already well investigated Co adatoms and dimers deposited on Pt(111) and compare them with their Fe analogues. These investigations are complemented by calculations for decorated clusters that allow to optimize the MAE. Our theoretical results are then used to simulate magnetisation curves of an ensemble of Fe_n $(n = 1, 2, 3)$ clusters on Pt(111), that are compared to recent experimental results.

2 Computational details

The calculations for the investigated cluster systems were done within the framework of spin density functional theory using the local spin density approximation (LSDA) with the parameterization given by Vosko, Wilk and Nusair for the exchange and correlation potential [16]. The electronic structure is determined in a fully relativistic way

[a] e-mail: hubert.ebert@cup.uni-muenchen.de

on the basis of the Dirac equation for spin-polarised potentials which is solved using the Korringa-Kohn-Rostoker (KKR) multiple scattering formalism [17,18]. This procedure consists of two steps. First the Pt(111) host surface is calculated self-consistently with the tight binding (TB) version of the KKR method using layers of empty sites to represent the vacuum region. This step is then followed by treating the deposited clusters as a perturbation to the clean surface with the Green's function for the new system being obtained by solving the corresponding Dyson equation. This scheme is described in more detail in earlier publications [12,13].

In all calculations the cluster atoms were assumed to occupy ideal lattice sites in the first vacuum layer and no effects of structure relaxation were included. Therefore, our results contain a systematic error and are strictly spoken not directly comparable with experimental data. Nevertheless, it could be shown already in earlier work [11, 13,14] on deposited clusters that this approach is capable of reproducing systematic trends as well as achieving a reasonable quantitative agreement with values found in experiment.

The $\alpha_{\hat{u}}$-component of the torque vector $T^{(\hat{n})}_{\alpha_{\hat{u}}}$ on the magnetic moments oriented along the direction $\hat{n}$ was calculated with an expression based on Lloyd's formula and perturbation theory [19]

$$T^{(\hat{n})}_{\alpha_{\hat{u}}} = -\frac{1}{\pi}\int dE\, f_{FD}(E) \times \mathrm{Im}\, i \sum_i \mathrm{tr}(\underline{\tau}^{(\hat{n})}_{ii}[(\hat{u}\cdot\hat{\underline{J}})\underline{t}_i{}^{(\hat{n})\,-1} - \underline{t}_i{}^{(\hat{n})\,-1}(\hat{u}\cdot\hat{\underline{J}})]). \quad (1)$$

Here f_{FD} is the Fermi distribution function, $\hat{u}$ is the direction of the torque vector and $\hat{J}$ is the total angular momentum operator. Finally, the matrices $\underline{t}_i{}^{(\hat{n})}$ and $\underline{\tau}^{(\hat{n})}_{ii}$ are the single site t-matrix and the site diagonal scattering path operator, respectively, where i (used as an index) labels the atomic sites. As the calculations are done assuming the temperature $T = 0$ K the Fermi distribution function is replaced by the theta function $\Theta(E_F - E)$ with E_F being the Fermi energy. For all results shown below, the energy integral $\int dE$ occurring in equation (1) was calculated on a rectangular complex energy mesh containing 64 points, while using an angular momentum expansion up to $l_{\max} = 2$ for all the occurring matrices.

Equation (1) uses the analytic derivative of the energy with respect to a rotation angle. We found that this approach is numerically much more robust than taking the differences between band or total energies. The disadvantage, however, is that the magnetic anisotropy energy, defined as the difference $E(\hat{n}, \hat{n}_0)$ of the energy for two orientations of the magnetisation, $\hat{n}$ and $\hat{n}_0$, respectively, has to be determined by a corresponding path integral:

$$E(\hat{n}, \hat{n}_0) = \int_{\hat{n}_0}^{\hat{n}} T^{(\hat{n})} d\hat{n}. \quad (2)$$

Developing $E(\hat{n}, \hat{n}_0)$ in spherical harmonics up to second order and taking into account the symmetry of the investigated cluster substrate systems, one finds for example for a cluster having C_{2v}-symmetry with respect to its spatial structure, i.e. ignoring the orientation $\hat{n}$ of the magnetisation [20]:

$$E(\theta,\phi) = E_0 + K_{2,1}\cos 2\theta + K_{2,2}(1-\cos 2\theta)\cos 2\phi + K_{2,3}\sin 2\theta \sin\phi. \quad (3)$$

Using a corresponding expression for the torque it is straight forward to deal with the integral occurring in equation (2). The evaluation of the anisotropy constants $K_{n,m}$ occurring in this equation can then be determined in a rather easy way by determining the torque for certain orientations $\hat{n}$ i.e. at angles (θ, ϕ) of the magnetic moments (see below).

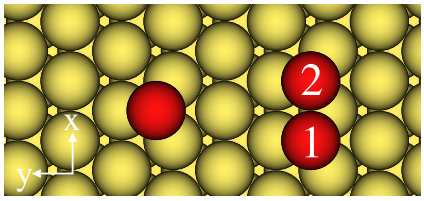

Fig. 1. Structures of the investigated systems: the cluster atoms occupy ideal lattice sites of the underlying Pt(111) substrate.

Table 1. Spin and orbital moments per atom of the investigated systems with magnetisation along the z-axis, i.e. perpendicular to the surface. For the mixed cluster the value refers to the component underlined.

	Co_1	Fe_1	Co_2	Fe_2	$\underline{Fe}Co$	$Fe\underline{Co}$
μ_{spin} (μ_B)	2.27	3.49	2.15	3.33	2.12	3.38
μ_{orb} (μ_B)	0.60	0.77	0.44	0.24	0.39	0.26

3 Results and discussion

The structure of the investigated Co and Fe monomers and dimers are shown together with the underlying Pt(111) substrate in Figure 1. As the ad- or cluster atoms, respectively occupy regular lattice sites correspondingly to the substrate the resulting cluster/substrate system has C_{3v}- and C_{2v}-symmetry, respectively. Comparing the resulting spin and orbital magnetic moments of Co and Fe in Table 1 one notices that the spin magnetic moments for Fe are in general about 1.5 times larger than for Co. For both transition metals the dimer formation has only a minor impact on their spin magnetic moments when compared to the single adatoms. The orbital moments, however, show a more interesting behaviour. Here we find already a substantial quenching when going from single adatoms to the corresponding pure i.e. unmixed dimers. This effect seems to be much more pronounced in the case of Fe where the orbital magnetic moment of a Fe_2 dimer atom reduces to about one third of the monomer value compared to only three quarters in the case of Co. The corresponding values for the mixed dimer differ only slightly from those of Co_2 and Fe_2, respectively. The different behaviour of the orbital moment for Co and Fe is also reflected in their anisotropies (see below). A further increase in cluster size leads usually (depending also on

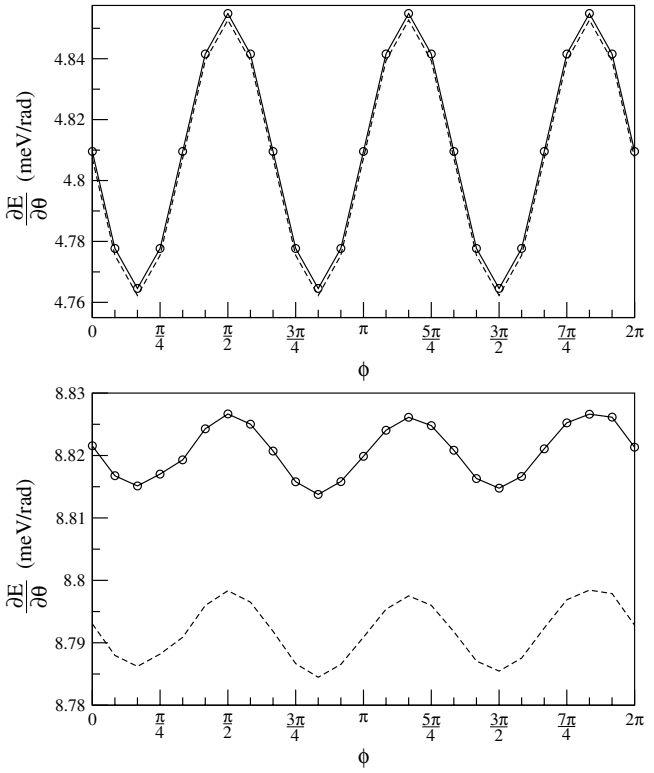

Fig. 2. Torque component $T_\theta(\theta, \phi)$ for Co_1 (top) and Fe_1 (bottom) at $\theta = \pi/4$ as a function of the azimuth angle ϕ (in fact $-T_\theta(\theta, \phi) = \partial E/\partial\theta$ is shown — see text). The dashed line shows the same results including the substrate effect.

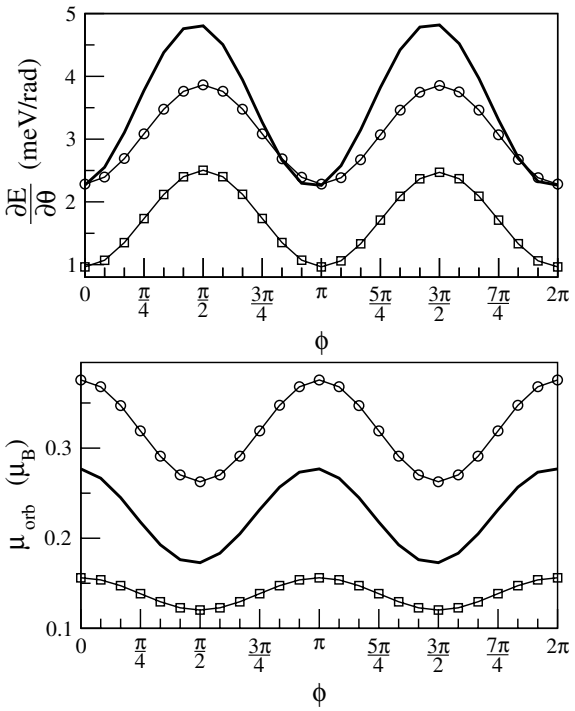

Fig. 3. Top panel: torque component $T_\theta(\theta, \phi)$ for Co_2 (circles), Fe_2 (squares) and the FeCo dimer (thick line) for $\theta = \pi/4$. Lower panel: ϕ dependence of the average orbital moments for all three dimers at $\theta = \pi/2$.

the cluster shape) to a rapid and monotonous decay of spin and orbital magnetic moments approaching rapidly the values of a monolayer. Obviously, this effect is caused by the increase in bandwidth of Fe and Co d-states upon increase of cluster size, while the differences observed for Fe and Co clusters are related to the different occupation of the Fe and Co d-bands.

Figure 2 shows the dependence of the θ-component of the magnetic torque $T_\theta(\theta, \phi) = -\partial E/\partial\theta$ on the azimuth angle ϕ for Co and Fe monomers at $\theta = \pi/4$. As $T_\theta(\theta, \phi)$ is found to be negative here as well as for the following we show always $\partial E/\partial\theta = -T_\theta(\theta, \phi)$. The positive sign of $\partial E/\partial\theta$ for all angles ϕ implies that the torque forces the magnetisation to the z-axis. This means that the system's easy axis points out of plane along $\hat{z}$. One can see that the threefold symmetry imposed by the underlying Pt substrate is directly reflected by the small oscillations of T_θ with the azimuth angle ϕ.

This also demonstrates the high sensitivity of our implementation. The curves show no numerical noise even for an energy resolution below 0.1 meV. As the ϕ dependence of T_θ is so small when compared to its absolute value the adatoms almost behave like perfect uniaxial magnets. In this case the anisotropy constants K can be extracted from the minima of $T_\theta(\theta, \phi)$. For the single adatoms this gives then 4.76 meV for Co and 8.79 meV for Fe. Figure 2 also shows the influence of the induced anisotropy coming from the Pt substrate atoms. This induced MAE is about -30 μeV for Fe and even smaller in the case of Co. In fact it seems to be negligible for very small Co clusters composed of only few atoms. For larger two-dimensional Co clusters, however, we found that this induced anisotropy becomes more important with increasing cluster size and can rise to the same order of magnitude as the contribution coming from the Co atoms themselves.

The results of the torque calculations for the three different investigated dimers are shown in the top panel of Figure 3. In all cases $\partial E/\partial\theta$ is again positive, however, the absolute values are significantly reduced when compared to the monomers. The ϕ-dependence of the θ-component of the torque on the other hand is now much more pronounced due to the reduced symmetry of the cluster/substrate system when compared to the monomer (see Fig. 1). From Figure 3 one can see that $E(\hat{n}, \hat{z})$ is smallest if the magnetic moments are oriented along the $\hat{x}$-direction, i.e. along the cluster dimer axis (see Fig. 1). The lower panel of Figure 3 shows the corresponding ϕ dependence of the orbital moments for $\theta = \pi/2$. One can see that the oscillations in the orbital moments follow the oscillations of T_θ in an anticyclic manner. Here it should be pointed out that the largest values for the orbital moments are obtained when the magnetisation points along the z-axis (see Tab. 1). This as well as the behaviour seen in Figure 3 is in qualitative agreement with the Bruno and van der Laan anisotropy models [21,22] that relate the MAE $E(\hat{n}, \hat{n}_0)$ to the corresponding anisotropy of the orbital moment.

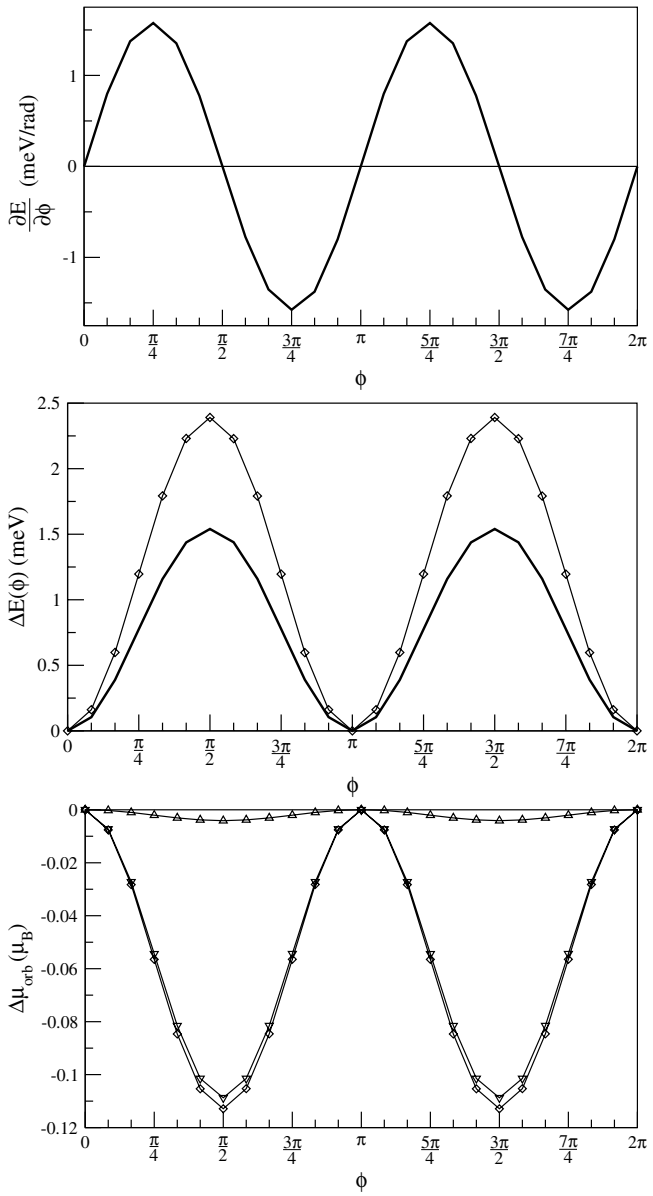

Fig. 4. Top panel: torque component $T_\phi(\theta,\phi)$ of Co_2 for $\theta = \pi/2$ as a function of ϕ. Middle panel: MAE $\Delta E(\phi)$ for $\theta = \pi/2$ referred to $\hat{n}_0 \mathrel{\hat{=}} (\pi/2, \phi = 0)$. The thick line gives calculated results while the thin line marked by diamonds gives results based on van der Laan's model. Lower panel: spin resolved anisotropy $\Delta\mu^{m_s}_{\rm orb}(\phi)$ for $\theta = \pi/2$ referred to $\hat{n}_0 \mathrel{\hat{=}} (\pi/2, \phi = 0)$ for spin up and down (triangles up and down, resp.) and summed up (diamonds).

For the van der Laan model one has

$$E(\hat{n},\hat{n}_0) = -\frac{\xi}{4\mu_B}[\mu^{\uparrow}_{\rm orb}(\hat{n}) - \mu^{\downarrow}_{\rm orb}(\hat{n})] + \frac{\xi}{4\mu_B}[\mu^{\uparrow}_{\rm orb}(\hat{n}_0) - \mu^{\downarrow}_{\rm orb}(\hat{n}_0)], \quad (4)$$

where ξ is the appropriate spin-orbit coupling constant (here for the $3d$ transition metal Fe or Co, respectively), and $\mu^{m_s}_{\rm orb}(\hat{n})$ is the spin projected orbital magnetic moment

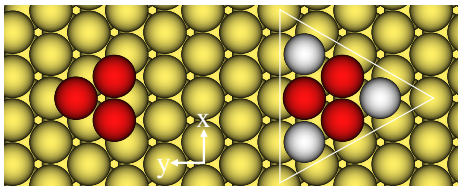

Fig. 5. Structure of the studied Fe trimer on Pt(111) without (left) and with (right) decoration by three Pt atoms.

for an orientation of the magnetisation along $\hat{n}$. If one considers a strong ferromagnet one can ignore the majority spin contribution in equation (4) leading to the expectation that the orbital magnetic moment takes its maximum for the magnetisation oriented along the easy axis. The results shown in Figures 2 and 3 are obviously in full agreement with this. As Figure 3 shows for the three considered dimers, also the MAE deduced from the shown torque goes parallel with the orbital magnetic moment (lower panel) when ϕ is varied while θ is kept fixed.

The relation of the MAE and the anisotropy of the orbital magnetic moment has been studied in more detail by calculating the ϕ-component of the torque for θ fixed to $\pi/2$, i.e. for the magnetisation forced to lie in the surface xy-plane. As one notes from the results given in Figure 4, the variation of the torque is again quite pronounced and reflects the C_{2v}-symmetry of the dimer/substrate system. Integrating the torque component with respect to ϕ (see Eq. (2)) one is led to the MAE $\Delta E((\pi/2,\phi),(\pi/2,\phi))$ shown in the middle panel of Figure 4, that again shows that the energy is at its minimum if the magnetisation lies along the dimer axis. The corresponding anisotropy $\Delta\mu_{\rm orb}(\phi)$ is given in the lower panel of Figure 4 in a spin-polarized way. As one notes the majority contribution to $\Delta\mu_{\rm orb}(\phi) = \mu_{\rm orb}(\pi/2,\phi) - \mu_{\rm orb}(\pi/2,0)$ is very small and negligible. This is a consequence of the nearly complete filling of the majority spin d-band of the Co-atoms, i.e. their strong ferromagnetic behaviour. As a consequence, one has not to distinguish between Bruno's and van der Laan's models. Using the relation given in equation (4) together with the spin orbit coupling strength $\xi = 85$ meV for Co [23] one is lead to the estimate for the MAE $\Delta E(\phi)$ in the middle panel represented by the curve marked by diamonds. Obviously, the qualitative behaviour of the MAE is properly reproduced with a reasonable quantitative agreement.

Figures 2 and 3 show that going from a monomer to a dimer the MAE is drastically reduced. This goes on with increasing cluster size, although there is some influence of the cluster shape [4]. As one notes, the decrease of the MAE is much more pronounced for Fe than for Co. For the mixed FeCo cluster, however, the MAE is quite high. This indicates that by a suitable combination of atoms one may optimize the MAE while keeping the magnetisation high. In fact, there are already a number of experimental studies done along this line. Here, we show results for the impact on the properties of a Fe trimer on Pt(111) due to a decoration with Pt atoms.

Figure 5 shows the corresponding structure of the investigated cluster/substrate systems. The resulting spin and orbital magnetic moments are given in Table 2. As one notes, the moments of the Fe atoms are again quite

Table 2. Spin and orbital moments per atom of the Fe_3 and Fe_3Pt_3 clusters on Pt(111) for the magnetisation along the z-axis, i.e. perpendicular to the surface. The values refer to the component underlined. The last two columns give results for the Pt-substrate atoms having one or two Fe atoms as nearest neighbours, resp., in case of Fe_3Pt_3.

	Fe_3	$\underline{Fe_3}Pt_3$	$Fe_3\underline{Pt_3}$	Pt(1)	Pt(2)
$\mu_{\rm spin}$ ($\mu_{\rm B}$)	3.20	3.16	0.21	0.09	0.11
$\mu_{\rm orb}$ ($\mu_{\rm B}$)	0.16	0.09	0.08	0.02	0.02

high as for the mono- and dimer. For the spin moment one finds only a minor influence due to the decorating Pt atoms. These have also quite an appreciable induced magnetic moment. The resulting torque $T_\theta(\theta,\phi)$ for $\theta = \pi/4$ as a function of the angle ϕ is shown in Figure 6 (top panel) for the Fe_2-, Fe_3- and Fe_3Pt_3 clusters. As is demonstrated once more the torque T_θ and with this also the MAE is strongly reduced going from the dimer to the trimer. Adding the decoration, however, the high MAE of the dimer is recovered. As the inner Fe_3 cluster of the Fe_3Pt_3 cluster is now surrounded by neighbouring atoms the variation of the MAE with ϕ is strongly reduced when compared with the dimer.

As one would expect, the MAE of the decorated trimer Fe_3Pt_3 is dominated by its Fe contribution. This can be seen in the middle panel of Figure 6 where apart from the total MAE per Fe-atom the averaged contribution of a Fe-atom is shown. Nevertheless, there is an appreciable contribution coming from the decorating Pt atoms as well. This has to be ascribed on the one-hand side to their appreciable induced magnetic moment (see Tab. 2) and on the other side to their large spin-orbit coupling ($\xi_{\rm Pt} = 710$ meV to be compared with $\xi_{\rm Fe} = 65$ meV). Apart from the contribution of the decorating Pt atoms there is a noteworthy contribution from the neighbouring Pt-substrate atoms as well. As can be seen in the lower panel of Figure 6 this amounts to about 5% of the total torque or MAE, respectively.

The results for the undecorated Fe_n clusters ($n = 1, 2, 3$) shown in the lower panel of Figure 2 and the top panel of Figure 6 allows us to make contact to our corresponding (so far unpublished) experimental investigations. The sample preparation technique used within these investigations is described in reference [24] and led to an ensemble of Fe_n clusters that was dominated by clusters of size $n = 1$–3 with their statistical weight determined to be $w_n = 0.53$, 0.54 and 0.33% (for the details of the evaluation procedure used for small clusters see e.g. Ref. [7]). Figure 7 shows the magnetisation curves $M(B)$ measured for this cluster ensemble at $T = 6$ K for an orientation of the external magnetic field $\boldsymbol{B}$ along the easy axis ($\hat{z}$) and at an angle $\theta \mathrel{\hat{=}} 65°$ with respect to this axis. With the theoretical magnetic moments and the anisotropy parameters for the Fe_n clusters available the magnetisation curves $M(B)$ can be simulated by means of the so-called Langevin formula [4]. This way the thermal average of the z-component $m_{nz}(B,T)$ of the moment m_n of an Fe_n

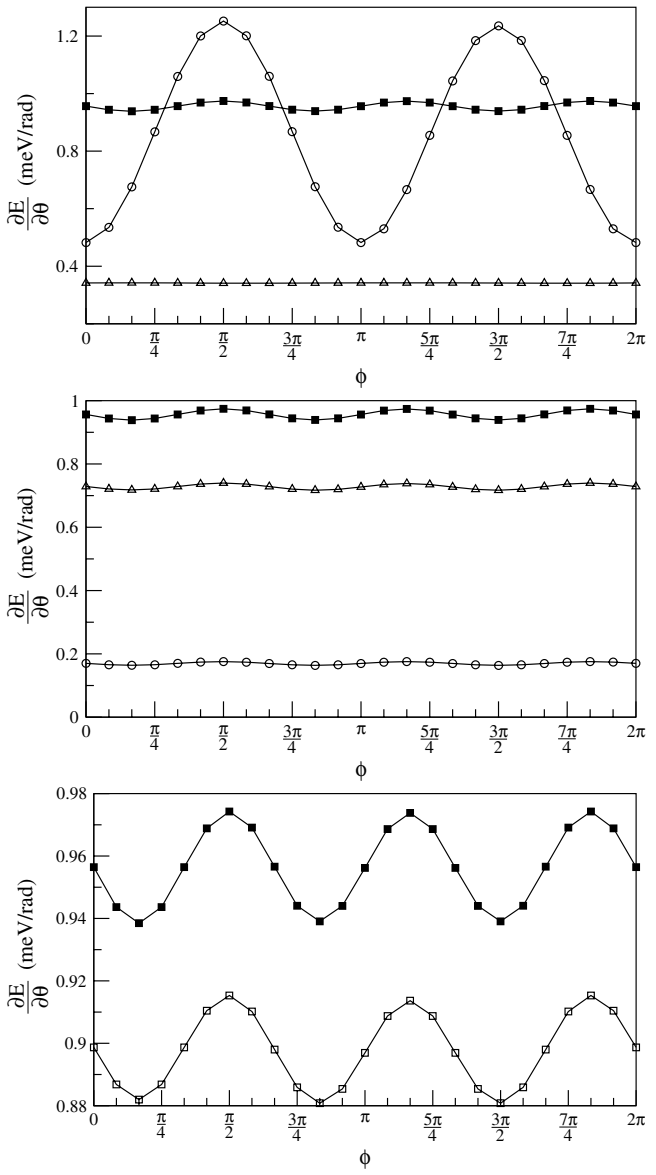

Fig. 6. Top panel: torque component $T_\theta(\theta,\phi)$ for Fe_2 (circles), Fe_3 (triangles) and Pt_3Fe_3 (squares) for $\theta = \pi/4$ as a function of the azimuth angle ϕ. Middle panel: torque component $T_\theta(\theta,\phi)$ per Fe atom for Pt_3Fe_3 at $\theta = \pi/4$ as a function of ϕ: total (full squares) including the substrate contribution, contribution of a Fe atom (triangle) and a cluster Pt atom (circles). Lower panel: total torque component $T_\theta(\theta,\phi)$ per Fe atom for Pt_3Fe_3 at $\theta = \pi/4$ as a function of the azimuth angle ϕ with (full squares) and without (open squares) the substrate contribution.

cluster can be expressed by:

$$m_{nz}(B,T) = \frac{\int_0^\pi \sin\theta d\theta e^{-E(B,T,\theta)/kT} m_n \cos\theta}{\int_0^\pi \sin\theta d\theta e^{-E(B,T,\theta)/kT}}. \qquad (5)$$

For the simulation the energy $E(B,T,\theta)$ was assumed to consist of its Zeeman and anisotropy contributions

$$E(B,T,\theta) = B m_n \cos\theta + K_1^n \sin^2\theta \qquad (6)$$

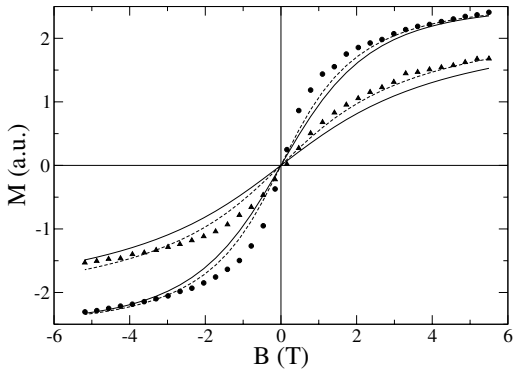

Fig. 7. Experimental magnetisation curves $M(B)$ (dots) of an ensemble if Fe_n clusters on Pt(111) measured at $T = 6$ K for an orientation of the magnetic field $M(B)$ along the easy axis $\hat{z}$ ($\theta = 0°$) and rotated by $\theta = 65°$ with respect to that. The full lines give corresponding theoretical results obtained on the basis of the calculated properties of Fe_n clusters and the Langevin formula given in equation (5). The dashed line is obtained by including Fe_4 clusters in the simulation.

where for the later one an uniaxial behaviour has been assumed. The corresponding anisotropy constant K_1^n has been deduced from the results for the MAE shown above. Adding the magnetisation curves for the Fe_n clusters weighted by their statistical weight w_n one is lead to the full lines shown in Figure 7. The additional dashed lines stem from a second simulation done including tetramers. This indicates that a certain amount of larger Fe clusters are formed during the preparation process as expected by statistics.

The good agreement of the simulated curves with experiment obviously demonstrates that the complex magnetic properties of transition metal clusters can indeed be understood and described without adjustable parameters on the basis of the approach used here. It also shows that inclusion of relaxation effects when calculating the cluster properties should only slightly modify the numerical results. Nevertheless, corresponding numerical works are in progress to determine the influence of lattice relaxations.

4 Conclusion

We have presented results for the magnetic anisotropy of various Co/Pt(111) and Fe/Pt(111) cluster/substrate systems calculated by the fully relativistic KKR-approach. It was demonstrated that calculating the magnetic torque instead of the magnetic anisotropy energy directly, is numerically very robust and reliable. This is in particular reflected by the accuracy achieved for the dependency of the torque on the azimuth angle ϕ as well as the results for the substrate contribution.

As in previous work it was found that increasing the cluster size leads in general to a rapid decrease of the MAE. However, it could be shown that by suitable formation of compound clusters this drop can be compensated. In fact, the combination of an element with large magnetic moments with one having large spin-orbit coupling seems to be a promising approach.

Finally, it could be demonstrated that using the calculated cluster properties the results of experimental magnetisation curves could be reproduced in a very satisfying way confirming the adequateness of our approach as well as the interpretation of the experimental findings.

We acknowledge support by the Deutsche Forschungsgemeinschaft within the Schwerpunktprogramm 1153 *Cluster in Kontakt mit Oberflächen: Elektronenstruktur und Magnetismus.*

References

1. J. Bansmann et al., Surf. Sci. Rep. **56**, 189 (2005)
2. G. Nicolas, J. Dorantes-Davila, G.M. Pastor, Phys. Rev. B **74**, 014415 (2006)
3. F. Meier, K. von Bergmann, P. Ferriani, J. Wiebe, M. Bode, K. Hashimoto, S. Heinze, R. Wiesendanger, Phys. Rev. B **74**, 195411 (2006)
4. P. Gambardella et al., Science **300**, 1130 (2003)
5. S. Rusponi, T. Cren, N. Weiss, M. Epple, B. Buluschek, L. Claude, H. Brune, Nature Mat. **2**, 546 (2003)
6. C. Petit, S. Rusponi, H. Brune, J. Appl. Phys. **95**, 4251 (2004)
7. P. Gambardella, A. Dallmeyer, K. Maiti, M.C. Malagoli, W. Eberhardt, K. Kern, C. Carbone, Nature **416**, 301 (2002)
8. P. Gambardella, S. Rusponi, T. Cren, N. Weiss, H. Brune, C.R. Phys. **6**, 75 (2005)
9. H. Brune, e-J. Surf. Sci. Nanotech. **4**, 478 (2006)
10. P. Gambardella, A. Dallmeyer, K. Maiti, M.C. Malagoli, S. Rusponi, P. Ohresser, W. Eberhardt, C. Carbone, K. Kern, Phys. Rev. Lett. **93**, 077203 (2004)
11. O. Šipr, S. Bornemann, J. Minár, S. Polesya, V. Popescu, A. Simunek, H. Ebert, J. Phys.: Condens. Matter **19**, 096203 (2007)
12. S. Bornemann, J. Minár, S. Polesya, S. Mankovsky, H. Ebert, O. Šipr, Phase Transitions **78**, 701 (2005)
13. J. Minár, S. Bornemann, O. Šipr, S. Polesya, H. Ebert, Appl. Phys. A **82**, 139 (2006)
14. B. Lazarovits, L. Szunyogh, P. Weinberger, Phys. Rev. B **67**, 24415 (2003)
15. Y. Xie, J.A. Blackman, Phys. Rev. B **74**, 054401 (2006)
16. S.H. Vosko, L. Wilk, M. Nusair, Can. J. Phys. **58**, 1200 (1980)
17. H. Ebert, *Fully relativistic band structure calculations for magnetic solids – Formalism and Application*, in *Electronic Structure and Physical Properties of Solids*, edited by H. Dreyssé (Springer, Berlin, 2000), Vol. 535 of Lecture Notes in Physics, p. 191
18. H. Ebert, R. Zeller, *The SPR-TB-KKR package*, `http://olymp.cup.uni-muenchen.de/ak/ebert/SPR-TB-KKR` (2005)
19. J.B. Staunton, L. Szunyogh, A. Buruzs, B.L. Gyorffy, S. Ostanin, L. Udvardi, Phys. Rev. B **74**, 144411 (2006)
20. B. Lazarovits, B. Ujfalussy, L. Szunyogh, G.M. Stocks, P. Weinberger, J. Phys.: Condens. Matter **16**, S5833 (2004)
21. P. Bruno, Phys. Rev. B **39**, 865 (1989)
22. G. van der Laan, J. Phys.: Condens. Matter **10**, 3239 (1998)
23. V. Popescu, H. Ebert, B. Nonas, P.H. Dederichs, Phys. Rev. B **64**, 184407 (2001)
24. D. Repetto et al., Phys. Rev. B **74**, 054408 (2006)